Muon-Induced Single Event Upsets in Deep-Submicron Technology

Brian D. Sierawski, *Member, IEEE*, Marcus H. Mendenhall, *Member, IEEE*, Robert A. Reed, *Senior Member, IEEE*, Michael A. Clemens, *Student Member, IEEE*, Robert A. Weller, *Senior Member, IEEE*, Ronald D. Schrimpf, *Fellow, IEEE*, Ewart W. Blackmore, *Member, IEEE*, Michael Trinczek, *Member, IEEE*, Bassam Hitti, Jonathan A. Pellish, *Member, IEEE*, Robert C. Baumann, *Fellow, IEEE*, Shi-Jie Wen, Rick Wong, and Nelson Tam

***Abstract*—Experimental data are presented that show low-energy muons are able to cause single event upsets in 65 nm, 45 nm, and 40 nm CMOS SRAMs. Energy deposition measurements using a surface barrier detector are presented to characterize the kinetic energy spectra produced by the M20B surface muon beam at TRIUMF. A Geant4 application is used to simulate the beam and estimate the energy spectra incident on the memories. Results indicate that the sensitivity to this mechanism will increase for scaled technologies.**

***Index Terms*—Direct ionization, Geant4, Monte Carlo, muons, single event upset (SEU), static random access memory (SRAM).**

I. Introduction

THE composition of terrestrial ionizing radiation is largely the result of cosmic ray showers in the Earth's atmosphere. High-energy protons and alphas create secondary particles as they bombard the atmosphere. After several generations of interactions, the sea level environment consists of neutrons, protons, pions, and muons, among other particle species. The contributions to the soft error rate (SER) for microelectronic devices due to alpha emission and thermal neutron capture can be managed, at least to some extent, through careful process control. Therefore, characterization of a device's response to fast neutrons, which cannot be mitigated, has provided an adequate estimation for the field SER. While terrestrial neutrons are quite numerous, 13 $cm^{-2}hr^{-1}$ above 10 MeV at New York City [1], they rarely interact with material.

Recently, research has shown that commercial static random access memories (SRAMs) are now so small and sufficiently sensitive that single event upsets (SEUs) may be induced from the electronic stopping of a proton [2]–[6]. This sensitivity appeared near the 65 nm technology node as the critical charge to upset a cell is on the order of 1 fC; merely 6 000 electrons are required to cause a change in data state. With continued advancements in process size, this downward trend in critical charge is expected to continue.

Muons, the most numerous terrestrial species, with a flux of nearly 60 $cm^{-2}hr^{-1}$ for momenta greater than 0.35 GeV/c [7], are also singly charged. Wallmark and Marcus provided a brief investigation of the role of these particles as one of the fundamental physical limits to continued microelectronic scaling [8]. Ziegler and Lanford provided a much expanded investigation of cosmic ray induced error rates and predicted the coming of a dramatic increase in errors with decreased critical charge [9]. The publication provides an excellent survey of the terrestrial particle environment and interactions that lead to charge generation in semiconductors. Burst-generation curves are used to evaluate the frequency of particle events leading to recoils of a given energy. The analysis of the relative contribution to the error rate for selected parts included the effects due to electrons, muons, protons, and neutrons through consideration of the ionization wake, recoils, alpha production, and capture. The authors predicted, although with limited environmental measurements, that devices with extremely low critical charge values will be susceptible to upset from, and errors dominated by, the muon ionization wake. While the history of process scaling has dramatically altered the device geometries, the crossover where this mechanism was predicted to exceed the neutron contribution was for devices with critical charges below 5 fC in [10].

Dicello published a series of papers comparing the muon and pion error counts and contribution to the sea level error rate [11]–[14]. In [11], the authors report on error counts measured with a 4K NMOS SRAM at LAMPF. The 164 MeV/c π^- beam was able to generate nearly 1000 errors, a 109 MeV/c μ^+ beam only produced 3 errors, and no errors were observed for the μ^- beam. The μ^+ errors were attributed to pion contaminants however. The author concluded that pions may be a major component of the sea level error rate. In [12] the authors obtained similar data, but used a lucite degrader in the beam line to mod-

Manuscript received July 16, 2010; revised September 10, 2010; accepted September 12, 2010. Date of current version December 15, 2010. This work was supported in part by Defense Threat Reduction Agency Grants HDTRA1-08-1-003 and HDTRA1-08-1-0034, the Defense Threat Reduction Agency Radiation Hardened Microelectronics Program under IACROs 09-4587l and 10-4977l to NASA, and the NASA Electronic Parts and Packaging Program.

B. D. Sierawski is with the Institute for Space and Defense Electronics, Vanderbilt University, Nashville, TN 37203 USA (e-mail: brian.sierawski@vanderbilt.edu)

M. H. Mendenhall, R. A. Reed, M. A. Clemens, R. A. Weller, and R. D. Schrimpf are with the Electrical Engineering and Computer Science Department, Vanderbilt University, Nashville, TN 37235 USA.

E. W. Blackmore, M. Trinczek, and B. Hitti are with TRIUMF, Vancouver, BC V6T2A3 Canada.

J. A. Pellish is with the NASA Goddard Space Flight Center, Greenbelt, MD 20771 USA.

R. C. Baumann is with Texas Instruments Incorporated, Dallas, TX 75243 USA.

S.-J. Wen and R. Wong are with Cisco Systems Inc., San Jose, CA 95134 USA

N. Tam is with Marvell Semiconductor Inc., Santa Clara, CA 95054 USA.

Digital Object Identifier 10.1109/TNS.2010.2080689

erate the energy. The pion-induced error counts decreased with increasing degrader thickness until the device entered the stopping region in which the π^- error counts increased over the π^+ by a factor of 7 because of π^- capture.

Dicello provided an estimate of SEU error rates at sea level and 10 km based on exposure of an NMOS SRAM to pions and muons [14]. The experiment used a cloud muon beam produced by pion decay to obtain error counts. By placing the device in the μ^- stopping region, the authors were able to measure three errors over the course of 24 hours. No errors were observed with μ^+. Based on this experiment, the stopping muon error rate was estimated at 2% of the total rate from all species. The authors also state that there are large uncertainties in the relative fluence of the terrestrial species.

While muon soft errors have been predicted by others, we present direct experimental evidence that microelectronics are susceptible to the muon ionization wake. In particular, a low-energy muon beam line was used to characterize 65 nm, 45 nm, and 40 nm CMOS SRAMs. We describe the beam line and characterization, the device response, and discuss the implications of low-energy muon sensitivity.

II. Energy Loss Mechanisms

The motivation for muon testing is to examine the ability of electronic stopping to produce single event upsets. Muons interact with material through the electromagnetic and weak forces. Muons may also decay to produce electrons, positrons, and neutrinos. However, these particles deposit little energy through electronic stopping or rarely interact. Negatively charged muons may be captured by a nucleus, however, μ^+ are not. Therefore, testing with low-energy μ^+ will examine the contribution of electronic stopping to SEU.

Although muons and protons have different masses, they are both singly-charged particles. The Bethe-Bloch equation for energy loss through electronic stopping indicates that the effect is primarily dominated by the charge and velocity of the particle. Therefore a muon with the same velocity as a proton will cause the same ionization. Fig. 1 shows the mass stopping power for a muon and proton in silicon. Whereas the Bragg peak for a proton in silicon is roughly 55 keV, it is approximately 8 keV for a muon.

III. Experimental Setup

To investigate the effects of low-energy muons on the reliability of microelectronics, we performed accelerated tests with the M20B beam line at TRIUMF [15]. This facility produces surface muons (positive muons from the decay of stopped pions near the surface of the production target [16]) for scientific research. A diagram of the beam line is shown in Fig. 2. The meson production begins with a 100 μA 500 MeV proton beam BL1A focused on the production target 1AT2 consisting of 10 cm of beryllium. Pions are produced within the target and decay with a lifetime of 26 ns into a muon and neutrino. Although both π^+ and π^- are produced, the π^- are mostly captured within

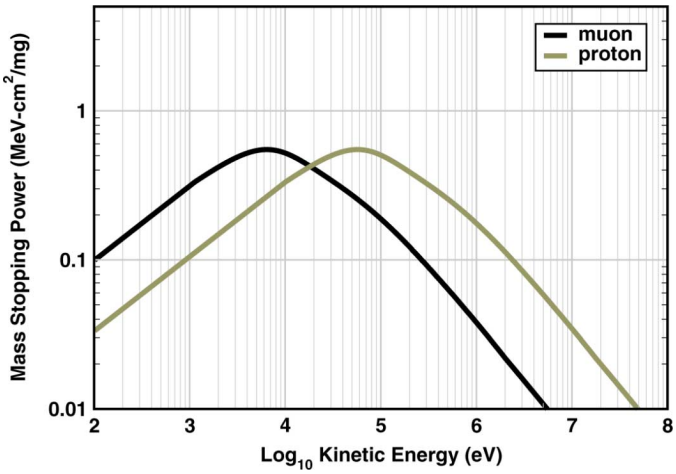

Fig. 1. Energy loss in silicon for muons compared with protons.

the target and do not decay into μ^-. The remaining μ^+ surface muons have an initial kinetic energy of 4.1 MeV (30 MeV/c momentum) and are transported downstream to the beam line. The facility provides the user control over a dipole magnet (M20B1) to select particle momentum, followed by variable-width slits (M20SL1) for refinement. Following a second bending magnet (M20B2), an electrostatic separator (M20BSEP) provides velocity selection. Finally, a second set of slits (M20BSL2) is used for collimation and the beam is brought to the final focus.

Given the momentum and velocity selections in the beam line and the energy deposition in a surface barrier detector (discussed in Section IV.A), the mass of the accelerated particles is known to be 106 MeV/c^2 with sufficient certaintly to distinguish from pions. Positively-charged particles of different mass such as pions (140 MeV/c^2) and protons (938 MeV/c^2) are clearly eliminated. For instance, 420 keV protons match the 28 MeV/c channel momentum but are deflected away in the electrostatic separator. Similarly, pions are removed by the separator and further decay with a mean decay length of about 2 m. After traversing the 20 m channel length all pions are eliminated.

Positrons, while deflected by the magnets and separators upstream, are present downstream in the beam from muon decay. These particles deposit very little energy through electronic stopping and rarely interact through annihilation. The fact that the final particles range out as expected and produce positrons when they decay shows that the beam indeed consists of μ^+. Final confirmation of particle species is provided by many muon spin rotation experiments [16] that look at the depolarization pattern of muons using a spectrometer.

To provide dosimetry, a collimator with a 2.5 cm diameter aperture was placed at the beam line window and a scintillator positioned 1 cm from the window. At full momentum, a flux of $2 \times 10^6 \mu^+ \mathrm{s}^{-1}$ can be obtained in a 4 cm $\times$ 3 cm spot size; however, as the momentum selection is reduced, the flux is reduced. The presence of the scintillator further lowered the mean beam energy and broadened the energy distribution as discussed in the following section. The device under test was placed at normal incidence 3 cm behind the scintillator.

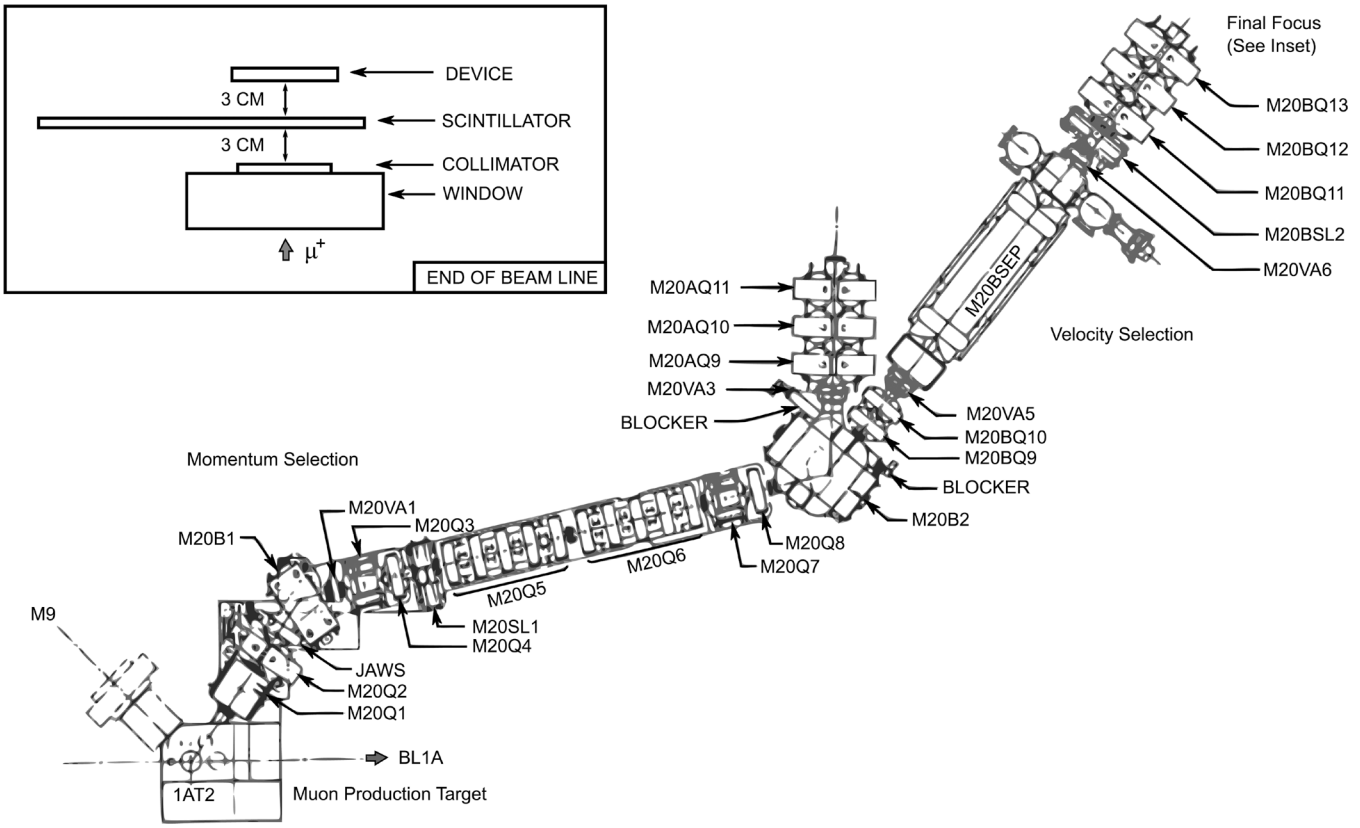

Fig. 2. The M20 beam line at TRIUMF selects muons through the use of bending magnets and an electrostatic separator [15]. Inset illustrates the position of test setup at the end of the beam line.

IV. Experimental Data

A. Surface Barrier Detector

To characterize the beam, a 500 μm thick fully-depleted surface barrier detector (SBD) was used in a pulse height analysis to measure the energy of the particles. The pulse height spectrum was calibrated with an alpha source. The detector was enclosed within an aluminum box 3 cm downstream of the scintillator with a 4 μm aluminized mylar window in the beam line. The detector was thick enough to stop all of the muons after the scintillator, so the SBD was an effective tool in characterizing the muon kinetic energy spectra. The dipole magnet M20B1 was adjusted to select muons with momentum lower than 28 MeV/c and the M20SL1 slits were opened to 20 mm. The M20BSL2 slits were not used during the test. The resulting energy deposition provides an adequate characterization of the kinetic energy as well as energy loss and straggling of the beam in the scintillator and other materials.

The top plot in Fig. 3 shows the deposited energy spectra as measured with the SBD at various momentum selections. At full momentum, the mean energy deposition in the SBD is slightly greater than 3 MeV whereas the initial kinetic energy is 3.6 MeV for a 28 MeV/c muon. This indicates that some energy has been lost in the passage through the materials between the final velocity selection and the device. As the momentum is decreased, the corresponding peak energy deposited by the stopping particles decreases. The low-energy contribution below 500 keV, which is seen in each spectrum, is most likely produced by positrons from μ^+ decay. With the magnet settings set to 21.6 MeV/c, the muon peak is barely distinguishable from the positron peak, and by 20 MeV/c the muon peak was completely indistinguishable. It is important to note that even though there are positrons in the beam, positrons cause significantly less energy deposition per unit path length than muons.

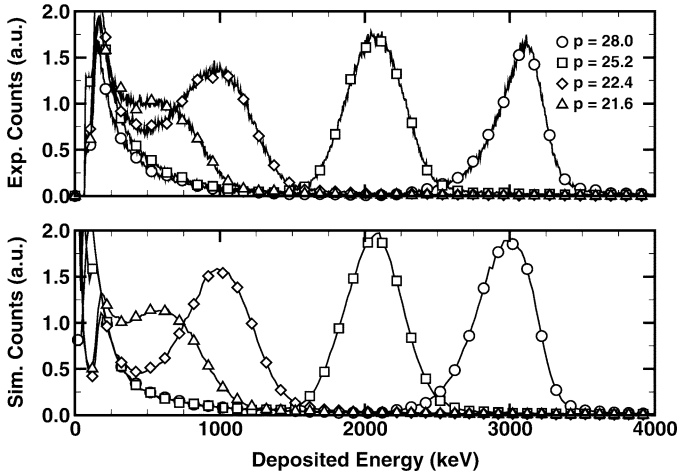

Fig. 3. Experimental (top) and simulated (bottom) energy deposition counts in 500 μm surface barrier detector.

A Geant4 application was used to investigate the energy deposition of muons in the detector. A muon beam with a 4% stan-

TABLE I
BASELINE ERROR COUNTS CHARACTERIZED VERSUS BIAS FOR 65 NM SRAM

Bias (V)	Runs	μ_B	σ_B
0.8	3	125.000	44.952
0.9	10	37.100	13.641
1.0	17	19.353	4.934
1.1	16	8.375	2.260
1.2	10	5.100	2.022

dard deviation in momentum was transported through a scintillator layer of CH_2 with an assumed thickness of 250 μm. Air gaps, the mylar window, and the SBD were included. Fig. 3 shows the results of the simulation compared with experimental data. Reducing the initial kinetic energy to the respective experimental condition and simulating the energy deposition in the SBD yields good agreement with measurements. The centroids shift appropriately and the positron contribution can be see in the low energy bins. The agreement of simulation results provides final confirmation that energy deposition at final beam focus is caused by the stopping of muons. This virtual beam line was used to interpret the SRAM results.

B. Static Random Access Memories

Two SRAMs used in this experiment were 8 Mbit test arrays fabricated in 65 nm and 45 nm commercial bulk CMOS processes. The third was a 5 Mbit array fabricated in a 40 nm bulk CMOS process. The 65 nm device overlayers were approximately 5 μm thick and the device was bonded as a chip-on-board to allow for front side testing. The 45 nm overlayers were approximately 7.5 μm. The 40 nm device overlayers were unknown. All SRAMs have been shown to upset with low-energy protons either in previous work [5] or in the Proton Irradiation Facility at TRIUMF. The 65 nm and 45 nm test boards are nominally biased at 1.2 V and operated by a "low cost" digital tester (LCDT) designed by the NASA Goddard Space Flight Center. The 40 nm test board was designed by Marvell and operated at 1.0 V. The 65 nm SRAM was characterized versus supply voltage with the beam off to establish a baseline for background errors. For each bias, the mean μ_B and standard deviation σ_B are reported in Table I. The other SRAMs did not experience background errors when operated at 1.0 V.

Data were collected over interspersed reads with the beam on and off to monitor any drift in the background errors. This baseline error count was verified to be independent of exposure time and is thought to be the result of unstable bits being operated below the recommended bias. Error counts in Table II are presented as the number of incorrect bits read exceeding the baseline errors. Error bars in Figs. 4 and 5 represent the standard deviation of the upset count after removing the measured distribution of baseline errors according to (1).

$$\sigma^2_{\mathrm{SEU}} = |N - \mu_B| + \sigma^2_B \tag{1}$$

A second set of Geant4 simulations was performed to characterize the muon kinetic energy spectra for the experimental momentum selections. In these simulations muons were transported through the scintillator and positrons were destroyed upon creation. The kinetic energy spectra at the surface of the SRAMs are shown in the bottom plot in Fig. 4. Given the prior agreement with the data acquired with the SBD, the simulation results provide a reasonable estimate of the incident beam.

The upset probabilities measured versus momenta are presented in the top plot of Fig. 4. The abscissa is related to the

TABLE II
SINGLE EVENT UPSET COUNTS FOR 65 NM SRAM

Bias (V)	P (MeV/c)	Runs	N	Muons ($\times 10^6$)	SEU (per $10^9\mu$)	σ_{SEU}
0.8	21.0	1	232	81.0	1321	569
0.8	22.4	1	179	113	478	403
0.9	21.0	1	89	100	519	154
0.9	21.6	1	70	56.0	588	264
1.0	19.6	3	62	144	27.3	60.8
1.0	20.4	3	86	204	137	49.3
1.0	21.0	6	204	461	191	33.2
1.0	21.6	4	175	382	255	36.5
1.0	22.4	3	88	357	83.9	28.4
1.0	23.8	3	59	493	1.91	17.4
1.0	25.2	1	28	232	37.3	24.8
1.0	28.0	1	17	326	-7.22	15.9
1.1	20.2	1	9	100	6.25	23.9
1.1	20.4	1	16	100	76.2	35.7
1.1	20.7	1	14	100	56.2	32.8
1.1	21.0	1	13	100	46.2	31.2
1.1	21.3	1	18	101	95.3	38.0
1.1	21.6	2	37	203	99.8	27.2
1.1	21.8	1	23	100	146	44.4
1.1	22.1	1	8	100	-3.75	23.4
1.1	22.4	1	13	101	45.8	30.9
1.2	19.6	1	7	53.0	35.8	46.2
1.2	21.0	1	8	74.0	39.2	35.7
1.2	21.6	2	19	427	20.6	9.7
1.2	22.4	2	11	211	3.79	14.2
1.2	23.8	1	7	165	11.5	14.8
1.2	25.2	1	2	224	-13.8	12.0
1.2	28.0	1	5	300	-0.33	6.8

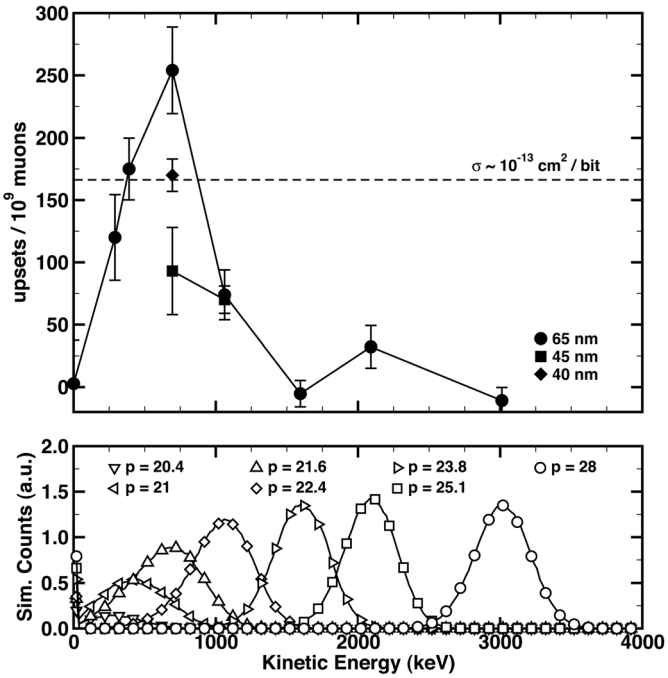

Fig. 4. Simulated muon kinetic energy distributions, as seen at the front of the part, corresponding to experimental momenta including upstream energy losses and straggling (bottom). Error counts for 65 nm, 45 nm, and 40 nm SRAMs versus estimated muon kinetic energy at 1.0 V bias (top). Dashed horizontal line represents an approximate muon-induced SEU cross section for reference.

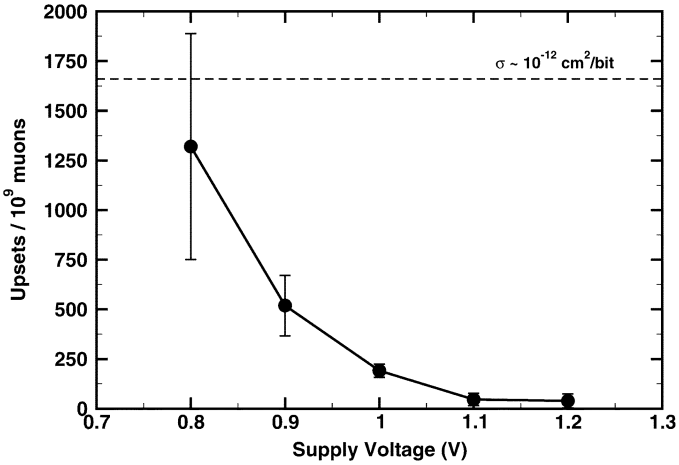

Fig. 5. Error counts for 65 nm SRAM versus supply voltage for approximately 400 keV muons produced by 21 MeV/c momenum selection. Dashed horizontal line represents an approximate muon-induced SEU cross section for reference.

kinetic energy by associating the upsets at the mode value of the simulated energy distribution. An approximate event cross section is indicated based on an estimate of the beam fluence. All SRAMs were operated at a supply voltage of 1.0 V. This bias was chosen because it produced a statistically significant error count.

At the highest energy, 3 MeV, the upset count was indistinguishable from the baseline for the 65 nm device. This was because muons pass through the device without generating sufficient charge to result in an SEU. Additionally, this measurement confirms that reported upsets cannot be attributed to noise sources while the beam is in operation. Near 700 keV the range of the beam through the metallization is such that a large portion of the muons traversing the active silicon are close to the Bragg peak and the collected charge is sufficient to exceed the critical charge. As the mean energy is further decreased, the beam begins to range out and the error counts return to the baseline. The 45 nm and 40 nm devices were spot checked and also exhibited muon sensitivities.

Fig. 5 shows the 65 nm device SEU response versus supply voltage for a distribution centered around 400 keV. At the nominal operating voltage of 1.2 V, few errors are attributed to muon upsets. However, as the voltage is reduced, the number of muon-induced upsets increases. The reduction in voltage corresponds to a reduction in critical charge. Therefore we expect that a greater range of muon energies are capable of inducing SEU at reduced bias.

V. Discussion

Accelerated testing with muons presents unique experimental challenges. First there are few high-energy facilities in the world that produce muon beams. Among these facilities, those that produce a surface muon beam are preferable to a cloud muon beam for observing a muon ionization effect. Surface muons are lower in energy since the pion decays within a production target and the construction of the following beam line reduces the possibility of contaminants reaching the device. Cloud and decay muons are produced by the decay of pions as they are transported down the beam line and can be either positive or negative polarity, but are typically higher energy. The range of the surface muons is limited because of the initial kinetic energy. Therefore, the amount of material encountered by muons must be reduced. This may require that a device be de-lidded and de-passivated for test. In addition to any kinetic energy spread, straggling causes a distribution of kinetic energies to reach the active device area.

Fortunately, if the part is insensitive to proton direct ionization, there is high confidence that it is also immune to muon direct ionization. Proton testing, unlike that for muons, is easier and accelerators are more readily available. If the device is sensitive to proton direct ionization, though, it is possibly also susceptible to muon ionization. The critical charge of present technologies is less than the muon ionization threshold. It is important to determine when (and if) muons will contribute a significant portion of the overall error rate. Testing a technology at reduced bias is a leading indicator for a sensitivity in scaled technologies.

VI. Summary

In this work, we report on measurements of single event upsets induced by muon electronic stopping. Accelerated testing shows an SEU error count that varies over beam energy in a manner that is consistent with the energy loss curve.

Accelerated neutron testing and soft error rate predictions are standard practices for terrestrial microelectronics applications with high reliability requirements. The data presented here, however, suggest that the SER of future technologies also may be affected by muons. Whereas neutrons only rarely interact with nuclei, both protons and muons are able to generate charge through the electromagnetic force. Therefore, the low-energy muon and protons fluxes have the potential to be a significant component of the SER for sensitive devices.

Our results suggest muon-induced upsets do not affect the soft error rate for 65 nm and 45 nm SRAMs operated at nominal supply voltage, but they are likely to have a greater impact for circuits fabricated in smaller process technologies with lower critical charge values. Ultimately, SRAMs, flip-flops, and combinational logic may become sensitive to the low-energy muon spectrum. Future terrestrial error rate predictions will require characterization of the device LET threshold, consideration of the muon environment, and advanced radiation transport computations.

Acknowledgment

The authors would like to thank personnel at the NASA Goddard Space Flight Center for their support, especially Kenneth LaBel, Michael Xapsos, Melanie Berg, Hak Kim, Mark Friendlich, and Christina Seidleck.

References

[1] "JESD89A: Measurement and reporting of alpha particle and terrestrial cosmic ray-induced soft errors in semiconductor devices," JEDEC Solid State Technology Assoc., 2006.

[2] D. F. Heidel, K. P. Rodbell, P. Oldiges, M. S. Gordon, H. H. K. Tang, E. H. Cannon, and C. Plettner, "Single-event-upset critical charge measurements and modeling of 65 nm silicon-on-insulator latches and memory cells," *IEEE Trans. Nucl. Sci.*, vol. 53, no. 6, pp. 3512–3517, Dec. 2006.

[3] K. Rodbell, D. Heidel, H. Tang, M. Gordon, P. Oldiges, and C. Murray, "Low-energy proton-induced single-event-upsets in 65 nm node, silicon-on-insulator, latches and memory cells," *IEEE Trans. Nucl. Sci.*, vol. 54, no. 6, pp. 2474–2479, Dec. 2007.

[4] D. Heidel, P. Marshall, K. LaBel, J. Schwank, K. Rodbell, M. Hakey, M. Berg, P. Dodd, M. Friendlich, A. Phan, C. Seidleck, M. Shaneyfelt, and M. Xapsos, "Low energy proton single-event-upset test results on 65 nm SOI SRAM," *IEEE Trans. Nucl. Sci.*, vol. 55, no. 6, pp. 3394–3400, Dec. 2008.

[5] B. Sierawski, J. Pellish, R. Reed, R. Schrimpf, K. Warren, R. Weller, M. Mendenhall, J. Black, A. Tipton, M. Xapsos, R. Baumann, X. Deng, M. Campola, M. Friendlich, H. Kim, A. Phan, and C. Seidleck, "Impact of low-energy proton induced upsets on test methods and rate predictions," *IEEE Trans. Nucl. Sci.*, vol. 56, no. 6, pp. 3085–3092, Dec. 2009.

[6] R. Lawrence, J. Ross, N. Haddad, R. Reed, and D. Albrecht, "Soft error sensitivities in 90 nm bulk cmos srams," in *Proc. IEEE Radiation Effects Data Workshop*, 20-24, 2009, pp. 123–126.

[7] P. K. Grieder, "Cosmic rays at sea level," in *Cosmic Rays at Earth*. Amsterdam, The Netherlands: Elsevier, 2001, pp. 305–457.

[8] J. T. Wallmark and S. M. Marcus, "Minimum size and maximum packing density of nonredundant semiconductor devices," in *Proc. IRE*, Mar. 1962, pp. 286–298.

[9] J. F. Ziegler and W. A. Lanford, "Effect of cosmic rays on computer memories," *Science*, vol. 206, no. 4420, pp. 776–788, 1979.

[10] R. Silberberg, C. H. Tsao, and J. R. Letaw, "Neutron generated single-event-upsets in the atmosphere," *IEEE Trans. Nucl. Sci.*, vol. NS-31, no. 6, pp. 1183–1185, Dec. 1984.

[11] J. F. Dicello, C. W. McCabe, J. D. Doss, and M. Paciotti, "The relative efficiency of soft-error induction in 4k static rams by muons and pions," *IEEE Trans. Nucl. Sci.*, vol. NS-30, no. 6, pp. 4613–4615, Dec. 1983.

[12] J. F. Dicello, M. E. Schillaci, C. W. McCabe, J. D. Doss, M. Paciotti, and P. Berardo, "Meson interactions in nmos and cmos static rams," *IEEE Trans. Nucl. Sci.*, vol. NS-32, no. 6, pp. 4201–4205, Dec. 1985.

[13] J. Dicello, "Microelectronics and microdosimetry," *Nucl. Instrum. Methods Phys. Res. B*, vol. B24–25, no. 2, pp. 1044–1049, 1987.

[14] J. F. Dicello, M. Paciotti, and M. E. Schillaci, "An estimate of error rates in integrated circuits at aircraft altitudes and at sea level," *Nucl. Instrum. Methods Phys. Res. B*, vol. B40, pp. 1295–1299, Apr. 1989.

[15] G. M. Marshall, "Muon beams and facilities at TRIUMF," *Zeitschrift fur Physik C Particles and Fields*, vol. 56, p. 226, Mar. 1992.

[16] J. H. Brewer, "μ + sr with surface muon beams," *Hyperfine Interact.*, vol. 8, no. 4, pp. 831–834, Jan. 1981.